RESEARCH ARTICLE | FEBRUARY 10 2016

Development of flexible SAW sensors for non-destructive testing of structure FREE

R. Takpara; M. Duquennoy; C. Courtois; M. Gonon; M. Ouaftouh; G. Martic; M. Rguiti; F. Jenot; L. Seronveaux; C. Pelegris

AIP Conf. Proc. 1706, 070003 (2016)
https://doi.org/10.1063/1.4940521

Development of Flexible SAW Sensors for Non-destructive Testing of Structure

R. Takpara[1, 2, a)], M. Duquennoy[1, b)], C. Courtois[2, c)], M. Gonon[3, d)], M. Ouaftouh[1, e)], G. Martic[4, f)], M. Rguiti[2, g)], F. Jenot[1, h)], L. Seronveaux[5, i)], and C. Pelegris[6, j)]

[1] *IEMN-DOAE, Université de Valenciennes, Le Mont Houy, 59313 Valenciennes, France.*
[2] *LMCPA, Université de Valenciennes et du Hainaut-Cambrésis, Pôle Universitaire de Maubeuge.*
[3] *UMONS, Université de Mons, Place du parc, 4 B7000 Mons – Belgique.*
[4] *CRIBC (membre d'EMRA), 4, Avenue Gouverneur Cornez, 7000 Mons, Belgique.*
[5] *SIRRIS, Liège Science Park, Rue du bois Saint-Jean 12, BE-4102 Seraing – Belgique.*
[6] *LTI-Université de Picardie Jules Verne-IUT de l'Aisne, France.*

[a)]Corresponding author: rafatou.takpara@univ-valenciennes.fr
[b)] marc.duquennoy@univ-valenciennes.fr
[c)] christian.courtois@univ-valenciennes.fr
[d)] Maurice.GONON@umons.ac.be
[e)] Mohammadi.Ouaftouh@univ-valenciennes.fr
[f)] g.martic@bcrc.be
[g)] mohamed.rguiti@univ-valenciennes.fr
[h)] Frederic.Jenot@univ-valenciennes.fr
[i)] Laurent.Seronveaux@sirris.be
[j)] christine.pelegris@iut.u-picardie.fr

Abstract. In order to accurately examine structures surfaces, it is interesting to use surface SAW (Surface Acoustic Wave). Such waves are well suited for example to detect early emerging cracks or to test the quality of a coating. In addition, when coatings are thin or when emergent cracks are precocious, it is necessary to excite surface waves beyond 10MHz. Finally, when structures are not flat, it makes sense to have flexible or conformable sensors for their characterization. To address this problem, we propose to develop SAW type of interdigital sensors (or IDT for InterDigital Transducer), based on flexible piezoelectric plates. Initially, in order to optimize these sensors, we modeled the behavior of these sensors and identified the optimum characteristic sizes. In particular, the thickness of the piezoelectric plate and the width of the interdigital electrodes have been studied. Secondly, we made composites based on barium titanate foams in order to have flexible piezoelectric plates and to carry out thereafter sensors. Then, we studied several techniques in order to optimize the interdigitated electrodes deposition on this type of material. One of the difficulties concerns the fineness of these electrodes because the ratio between the length (typically several millimeters) and the width (a few tens of micrometers) of electrodes is very high. Finally, mechanical, electrical and acoustical characterizations of the sensors deposited on aluminum substrates were able to show the quality of our achievement.

INTRODUCTION

Surface acoustic waves (SAW) are particularly suited to effectively monitoring and characterizing structural surfaces (condition of the surface, coating, thin layer, micro-cracks...). Conventionally, in non-destructive testing, wedge sensors are used to generate guided waves but they are especially suited to flat surfaces and sized for a given type material (angle of refraction). In addition, these sensors are quite expensive so it is quite difficult to leave the sensors permanently on the structure for its health monitoring. Therefore, we are considering in this study, another

42nd Annual Review of Progress in Quantitative Nondestructive Evaluation
AIP Conf. Proc. 1706, 070003-1–070003-9; doi: 10.1063/1.4940521

type of ultrasonic sensors, able to generate SAW. These sensors are interdigital sensors or IDT sensors for InterDigital Transducer [1-3]. This paper focuses on optimization of flexible IDT sensors, able to adapt to the geometry of structures, for non-destructive structural testing, using composite piezoelectric material. The challenge was to optimize the dimensional parameters of the IDT sensors in order to efficiently generate surface waves. Acoustic tests then confirmed these parameters.

CERAMIC FOAM

Our requirements concerning the IDT sensors lead us to use soft materials with good piezoelectric performance for the generation of surface waves. Certainly, there are some flexible materials such as PVDF (polyvinylidene fluoride), but despite its good mechanical properties, it has low piezoelectric properties [4,5]. Piezoelectric ceramic has high piezoelectric constant but they are rigid. In order to have flexibility we choose to use ceramic foam. So by introducing pores we will make piezoelectric ceramic be flexible.

Manufacturing Process of Porous Material

There are several methods for the development of porous materials. The choice of method is guided by the desired outcome (pore size, connectivity, porosity rate…). The main methods used are: replica method, the sacrificial template method and direct foaming method [6]. The latter method is the one used in this paper. Porous materials are produced by incorporating air into a suspension. The latter is subsequently set in order to keep the structure of air bubbles created, and dry (Figure 1):

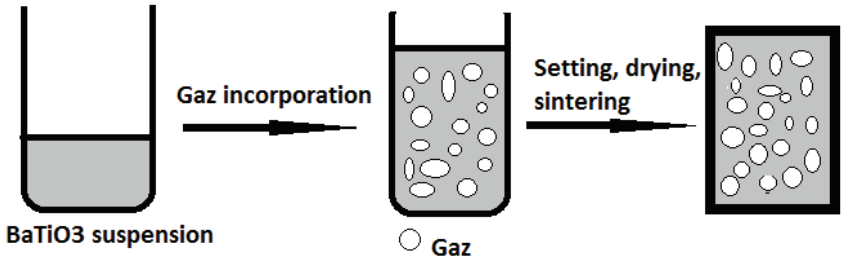

FIGURE 1. Direct foam method

The delicate step is the stabilization of foams. The stabilization of these foams is performed by the introduction of amphiphilic molecules (e.g., butyric acid)) [7, 8]. These molecules contain a hydrophilic head and a hydrophobic tail. The pH is adjusted so that the amphiphilic molecule adsorbs through its polar part, to the surface of the particles of $BaTiO_3$. The aim is to make the particles hydrophobic $BaTiO_3$ enough to drive to their adsorption to the air / water interface. To obtain high-strength porous ceramics, the consolidated foams are afterwards sintered at high temperatures. During sintering, the material is susceptible to cracking. It is therefore necessary to heat gradually as a temperature gradient would cause stresses and therefore cracks. The temperature profile is composed of three steps: heating to 1400°C with heating rate of 1°C/min, plateau of 2h at 1400°C followed by the natural cooling of the furnace (Figure 2).

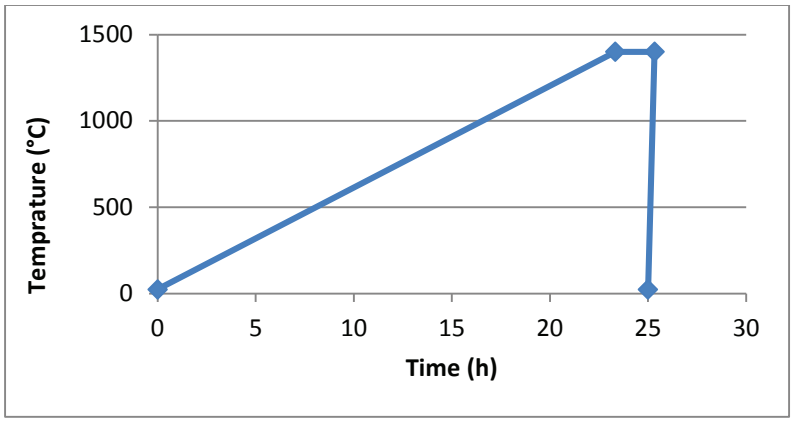

FIGURE 2. Sintering cycle of $BaTiO_3$ foam

The total porosity of directly foamed ceramics is proportional to the amount of gas incorporated into the suspension during the foaming process. Contrariwise the pore size is determined by the stability of the wet foam before setting takes place.

Characteristics of Ceramic Foams

By varying the concentration of butyric acid, it is possible to vary two parameters: porosity rate and pore size. The more the acid concentration is high, the less pores sizes are [9]. The stirring speed during the incorporation of gas also can influence on the pore size. The more the speed is high, the less pores size are. Today, we get to elaborate foams with porosity rate of 50 to 90%, and a pore size of between 50 µm and 100 µm. The developed foams have good piezoelectric properties with d_{33} up to 170pC / N (d_{33} = 26pC/N for PVDF, Table 1). However, the mechanical properties (in terms of flexibility) of foams remain low. Indeed, the relative deformation at rupture is low (er=0.13%) To remedy this fragility, we opted for the impregnation of foams by polymers.

Injection polymers found in the literature are: poly ε-caprolactone, urea-urethane elastomer and époxyl vinyl ester resin. In our case, we chose epoxy impregnation resin-type (trade name Epofix). It should be noted that the incorporation of polymer improves mechanical property without much altering the d_{33} of the material. Figure 3 presents the behavior of these two types of materials for mechanical stressing (bending). We find that the composite $BaTiO_3$/resin deforms more before rupture, contrary to the porous material. Some mechanical constants presented in Table 1, are used to compare the performance of the foam before impregnation and after impregnation (composite).

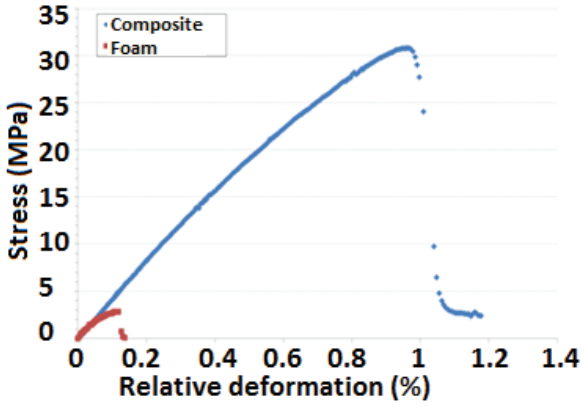

FIGURE 3. Bending tests of foam and the corresponding composite

TABLE 1. Mechanical properties of foam, $BaTiO_3$ composite, PVDF and the massif $BaTiO_3$.

Material	σ_r (MPa)	e_r (%)	E (GPa)	d_{33} (pC/N)
Foam	2.8	0.13	2.2	170
Composite	31	0.96	3.2	50-170
PVDF [10]	~60	~50	~2	26
$BaTiO_3$ (Bulk) [11]	-	< 0.1	80	190

OPTIMIZATION OF THE PARAMETER OF SAW SENSORS

An IDT sensor consists of two comb-shaped metal electrodes (often made of gold or silver) composed of interlinked fingers deposited on a piezoelectric plate (Figure 4). When a voltage "U" is applied between the two electrodes, the field created generates compressions and dilatations near the surface of the piezoelectric plate, thus producing surface waves. These waves are emitted each side of the sensor with a wave front parallel to the IDT sensor electrodes [12, 13].

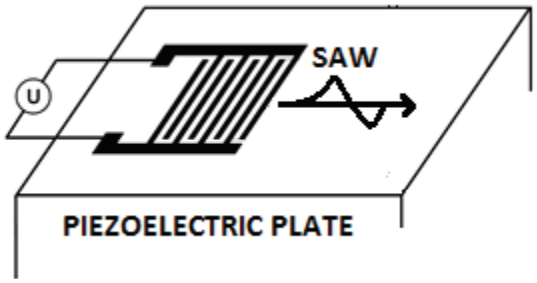

FIGURE 4. Diagram of an IDT sensor

The IDT sensor parameters were optimized to achieve significant levels of displacement compatible with non-destructive testing. This optimization was performed using COMSOL Multiphysics® finite element analysis software. With the finite element method, the solution space is discretized into subdomains called elements. These elements are the elementary bricks and the mesh represents the geometrical system to be simulated. The elements are composed of several nodes. Linear quadrangular elements were used as they provide a uniform mesh. Concerning the size of these elements, various tests have shown that sizes smaller than or equal to "$\lambda_R/10$" are required to obtain good results (where λ_R is the wavelength of SAW). A time step equal to "T/20" was selected, where T is the period of the electrical excitation signal. The full computation time T_c was calculated by adding the time of the electrical excitation signal to the propagation of the SAW waves in the plate. The propagation of the waves can thus be observed in the structure. The model used consists of the piezoelectric plate on which the SAW is generated, and two dampers located on either side. The thickness "e" of the plate was chosen to be sufficiently large in relation to the wavelength ($e \approx 10.\lambda_R$) to be in the right conditions for Rayleigh wave propagation. Finally, there are five pairs of electrodes on the piezoelectric plate. Bidirectional IDT sensors are considered and the width of the electrodes is equal to a quarter of a wavelength ($a = \lambda_R/4$). Electrodes are spaced half a wavelength apart, which corresponds to the central operating frequency ($a+b = \lambda_R/2$, where "a" is the width of electrode and "b" is the spacing between the electrodes). Normal displacements generated by the surface wave propagating on ceramic foam plate are shown in figure 5. Ceramic foams are thus able to generate surface acoustic waves.

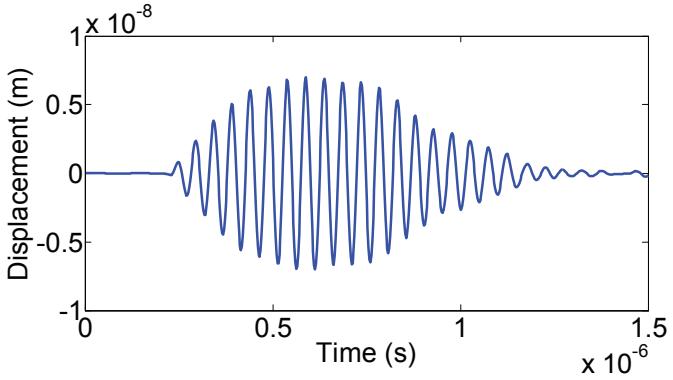

FIGURE 5. Normal displacements (in Y direction) generated on a piezoelectric plate

For the generation of SAW on the substrate, we use another model which consists of a piezoelectric plate glued to a substrate on which the SAW needs to be propagated. As before, two dampers were positioned at both ends of the substrate to prevent the unwanted return of waves propagating at the left end of the piezoelectric plate, and the two ends of the substrate (Figure 6). These precautions are necessary in the model, as the surfaces modeled are very small (number of nodes). However, the plate and the substrate are big enough in the experimental phase and there are no harmful wave reflections. "e" is the thickness of the piezoelectric plate, "e'" the thickness of the substrate and "P_1" the point on the substrate where the displacements are recorded.

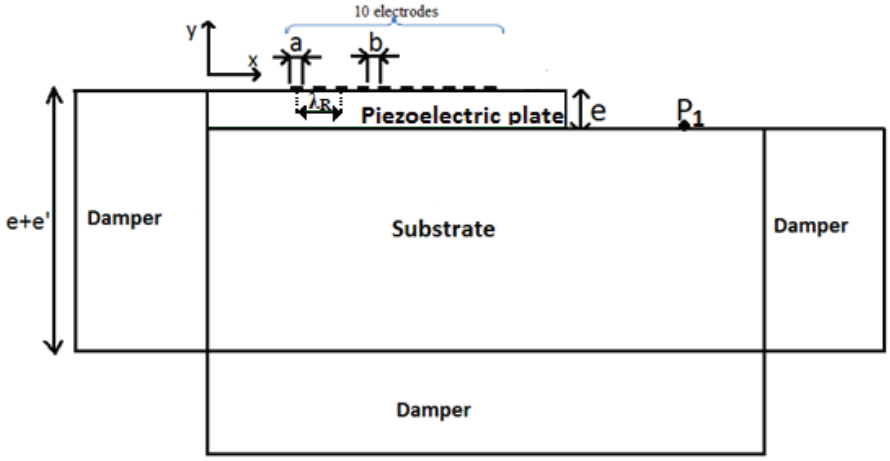

FIGURE 6. Model for simulating SAW on a piezoelectric plate bonded to substrate

Different thicknesses were tested to determine the optimum thickness for the generating of SAW on the substrate. Normal displacements depending on the piezoelectric thickness were recorded. From the simulation results, we observe three cases: the case corresponds to the case where the thickness "e" is very small relative to the surface wavelength, the case when "e" is comparable to that wavelength, and the case corresponds to the case where "e" is much larger than the wavelength in the piezoelectric plate. For the first case ($e << \lambda_R$), on one hand displacements generated on the substrate have small amplitudes. On other hand these thicknesses can be smaller than pores of foams, so they are not compatible with our piezoelectric material. So it won't make sense working with theses thicknesses. The second case ($e \approx \lambda_R$) is favorable to SAW excitation. Indeed, when a voltage is applied between the electrodes, a displacement field is immediately created throughout the thickness of the plate. The displacements are transmitted to the substrate and with each electrical impulse wave forms at the interface, then, the SAW progresses beyond the piezoelectric plate, on the substrate. In this interval, displacement amplitudes are high. Effective SAW generation is also confirmed by the shape of the displacement signal that is the same at any point on the substrate on one hand and looks like displacement signal presented at figure 5 on other hand. Finally, for the case 3 ($e >> \lambda_R$), SAW are strongly influenced by the piezoelectric plate edge because SAW are first generated on the plate, then bypass the edge of the plate, and finally propagate on the substrate. . These results are strongly dependent on the quality of the edge of the

blade. Since this element will be very difficult to control experimentally, we have not included this third case. In addition, displacements generated have small amplitudes. In conclusion, to generate effectively SAW on a substrate, the thickness of the piezoelectric plate must be comparable to the wavelength.

INTERDIGITATED ELECTRODES DEPOSITION

Laser Ablation Techniques

Laser ablation-based techniques are rapid, contactless and can be used to produce complex electrode patterns easily. Moreover, they can be edited at will as the laser spot vaporizes the metal areas where the metal needs to be removed, without having to resort to the use of masks (as with lithography). However, it is necessary to metalize the surface. Furthermore, local heating of the machined structure may occur, which can be detrimental (Curie temperature). The ideal would be to sublimate the layer without heating the substrate. This depends on the thermal conduction of the layer and the substrate, and the electromagnetic absorption of the layer. Finally, the technique used to prepare the metal coating, and the roughness of the surface of the substrate, involves more or less significant interpenetration of the coating in the substrate. These conditions will influence the ease of removing the metal layer. Finally, according to the characteristics of the coating and the substrate, and of the energy of the laser spot, there may be side effects of varying degrees.

The laser technique tested for manufacturing IDT sensors was a system equipped with an excimer-type laser (provider: Optec, equipment that is also part of the Hainolase platform), emitting a laser beam at 248 nm generated by photonic pumping through a gas mixture (Kr+F). The size of the output beam was 3x3 cm^2. The maximum power for a 6-ns pulse was 3 MW. The laser beam can be focused (~10X) using a set of optical lenses and with masks in the beam path can reach resolutions in the order of 25 µm. The technique produced interdigital electrodes with smaller widths than the previous ablation techniques. For the first tests, sensors that can theoretically transmit at frequencies of around 10 MHz were produced (scan rate = 20 mm/s and frequency = 200 Hz).

Ten minutes were necessary to prepare these sensors, as well as multiple masks (various sizes depending on the surface to ablate). Manufacturing a mask corresponding to the sensor to be "printed" and placing it at the laser beam outlet, would save a lot of time as only a few laser "shots" would be required to create the sensor. However, variations in ablation depth were observed because the energy density at the surface of the sample varied depending on the size of these masks. One possibility for this work would be to build a mask corresponding to the complete drawing of the sensor. This solution would enable the illumination of the entire surface and thus the ablation of all the areas at the same time in seconds (a few laser "shots" would be sufficient through the mask without having to move the xy table support. The sample would then receive the same energy per unit area (or energy density), and therefore the ablation depth would be the same everywhere and controlled better. The current method requires a compromise between sufficient ablation over large areas (larger size masks require more energy) and excessively deep ablation when smaller masks are used in order to obtain the best resolution. First, these complex masks need to be prepared. Finally, studies are currently underway to further improve the resolution for this type support.

Conductive Ink Printing Technique

Conductive ink printing processes are currently under development, particularly in the field of electronics. The main processes considered are high-speed manufacturing processes to produce conductive polymer-based plastic electronic components. Aerosol Jet Printing (AJP) is a high-resolution material deposition technique for printed electronics. Its distinctiveness consists in depositing atomized droplets of an ink filled with nano-scale particles. The benefits of this technology, besides making IDT sensors without a mask, are its multi-material, fine-line printing capability (Ag, Au, dielectric, semiconductor ink etc.). Furthermore, it has the ability to print conformal patterns over three-dimensional substrates and increase the thickness of the electrodes by local multilayer printing. For instance, the solution is very useful for making IDT connection pads. This capability of implementing local variations in coating thickness is also conceivable with current photolithographic processes. However, with the latter, there are many redundant critical operations involved in making multi-thickness coatings. Indeed, the time consuming "Lift off" process needs to be carried out several times and much care is required, particularly during the alignment step. Lastly, with AJP, local sintering of the deposited material by IR laser is possible. However, the stability of this process is highly dependent on the printing environment. Moreover, the porosity and the roughness of the substrates affect the deposition quality. Finally, as this process is based on line-by-line printing, defects such as spitting can occur resulting

in short-circuiting and destruction of the sensor. The sensors were produced on a commercial OPTOMEC® AJP300CE device. When the printing environment is controlled, this machine can achieve lines 10 µm wide and 150 nm thick in one step.

In order to produce a functional high-frequency IDT sensor, we have to use a process that can make high-resolution electrodes while guaranteeing the electrical continuity of the tracks. Moreover, the curing needed according to the implementation process chosen must not alter the substrate polarization. In the present study, we first focused on searching for the most appropriate production settings (tip choice, temperature, pressure…) to determine the limitations of AJP in manufacturing IDT on substrates. Indeed, the right parameters change according to the ink-substrate wetting, the roughness of the substrate, etc. In these trials, we decided to use ink loaded with silver nanoparticles because of its ease of use and its satisfactory electrical conductivity properties. We first noticed that the main difficulties were linked to the roughness and the porosity of the materials. Some issues with electrical continuity arose due to the absorption of the first ink deposit on the substrate. Indeed, it seems that the final thickness of the first layer was not thick enough to provide uninterrupted tracks throughout the whole electrode.

EXPERIMENTAL RESULTS

Various sensors have been achieved with piezoelectric composite ($BaTiO_3$/resin) plates. Different thicknesses have been tested (250µm , 300µm , 500µm, 1mm, 2mm) and different Eigen frequencies of 1 to 10 MHz. Figure 7 presents an example of IDT electrodes achieved on the piezoelectric $BaTiO_3$/resin composite. On the left side, the picture shows the interdigital electrodes produced by an excimer laser on a composite with a thickness of 500µm.There were twenty interdigital fingers with a length of 8mm and with a width of 150µm. On the right side, a SEM picture shows the quality of the ablation performed by the laser and the proportions, by the different shades of the three materials. Resin is Black, piezoelectric $BaTiO_3$ is dark grey and the electrode (platinum) is grey.

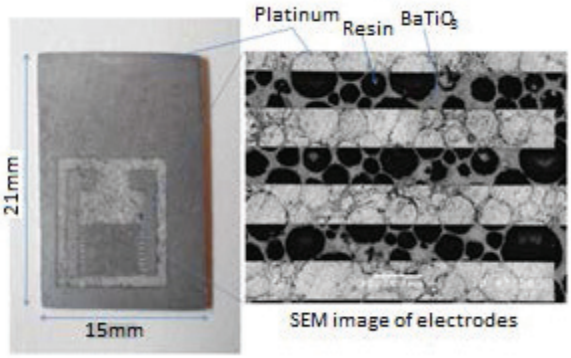

FIGURE 7. Achievement of IDT electrodes on a piezoelectric composite $BaTiO_3$/resin

The performances of these IDT sensors were acoustically tested. Figure 8 shows an example of SAW generated by a composite $BaTiO_3$/resin IDT sensor and detected on an aluminum substrate. Moreover, by measuring the delay time of the surface wave at several points, it was possible to confirm that the wave generated on aluminum was an SAW. This value is 2863 m/s. Displacements generated by IDT sensors and detected by a laser interferometer (Figure 8) are the same as in modeling. However, the amplitudes detected by the interferometer are very low, compared to those recorded by modeling. This may be caused by attenuation that was not considered in modeling. The presence of a resin (polymer) can produce an important attenuation and reduce the amplitude of displacements.

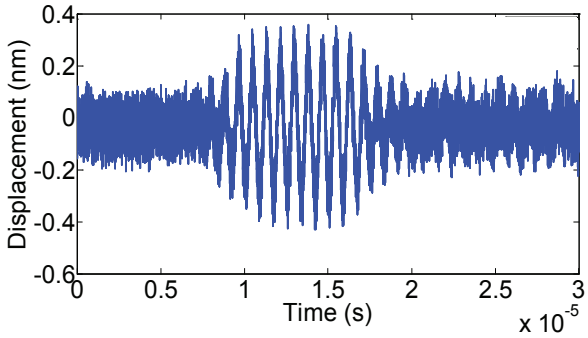

FIGURE 8. SAW generated on aluminum substrate using composite $BaTiO_3$/resin IDT sensor at 1,2MHz and detected by laser interferometer

CONCLUSION

This study aims to develop flexible interdigital transducers to generate surface waves in the CND. In this work, we have developed a composite piezoelectric material: foam impregnated by resin. This material being flexible, it is possible to use it on a non-flat surface. After, we have shown the ability of these piezoelectric foams to generate surface waves (by modelling and experimentally). We have shown that the thickness of the piezoelectric plate used to produce the IDT sensor must be comparable to the wavelength in the piezoelectric plate. Finally, we have shown the effectiveness of the IDT sensors by measuring the displacements caused by the surface wave on Aluminum substrate, even if the amplitude of displacements is small because of the attenuation of the resin. Thus, NDT testing with these flexible IDT sensors can be considered.

ACKNOWLEDGMENTS

We would like to thank Nord-Pas-de-Calais and the European Union (FEDER funds) for supporting our research through the CISIT and Interreg IV PRISTIFLEX program.

REFERENCES

1. J. Jin, S.T. Quek, Q. Wang, Design of interdigital transducers for cracks detection in plates, Ultrasonics 43 pp. 481–493 (2005).
2. J. K. Na, James L. Blackshire, Interaction of Rayleigh waves with a tightly closed fatigue crack, NDT&E International 43 pp. 432–439 (2010).
3. M. Duquennoy, M. Ouaftouh, J. Deboucq, J.E. Lefebvre, F. Jenot, M. Ourak, Characterization of micrometric and superficial residual stresses using high frequency surface acoustic waves generated by interdigital transducers, J. Acoust. Soc. Am. 134, 6 pp. 4360-4371 (2013).
4. M. Martins, V. Correia, J.M. Cabral, S. Lanceros-Mendez, J.G. Rocha, Optimization of piezoelectric ultrasound emitter transducers for underwater, Communications, Sensors and Actuators A 184 (2012) pp. 141– 148 (2012).
5. M. Castaings, Monkhouse, R. S. C.; Lowe, M. J. S.; Cawley, P., The Performance of Flexible Interdigital PVDF Lamb Wave Transducers, Acta Acustica united with Acustica, Volume 85, Number 6, pp. 842-849(8) (1999).
6. A. Studart, U. Gonzenbach, E. Tervoort, J. Gauckler, Processing Routes to Macroporous Ceramics: A Review, Journal of the American Ceramic Society, vol.89, issue 6, pp. 1771-1789 (2006).
7. U. Gonzenbach, A. Studart, E. Tervoort, and J. Gauckler, Macroporous Ceramics from Particle-Stabilized Wet Foams, Journal of the American Ceramic Society vol.90, issue 1, pp. 16-22 (2007).
8. P. Sepulveda and J. G. P. Binner, Processing of Cellular Ceramics by Foaming and In Situ Polymerisation of Organic Monomers, J. Eur. Ceram. Soc., 19 pp. 059–66 (1999).
9. U. Gonzenbach, A. R. Studart, Elena Tervoort, and Ludwig J. Gauckler, Stabilization of Foams with Inorganic Colloidal Particles, Langmuir 22, pp. 10983-10988 (2006).

10. Daniel M. Esterly, Manufacturing of Poly(vinylidene fluoride) and Evaluation of its Mechanical Properties, Masters of Science in Materials Science and Engineering, Blacksburg, Virginia (2002).
11. K. A. Vashishth, Vishakha Gupta, Wave propagation in transversely isotropic porous piezoelectric materials, International Journal of Solids and Structures 46 pp. 3620–3632 (2009).
12. D. Royer, Dieulesaint E., Elastic waves in solids I, Free guided propagation, Springer, (2000).
13. Royer D., Dieulesaint E., Elastic waves in solids II, Generation, acousto-optic interaction, applications, Ed. Springer, (2000).